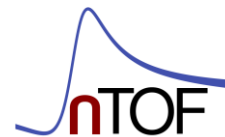


$^{33}\text{S}(n,\alpha)^{30}\text{Si}$ cross section measurement at n_TOF EAR2

Javier Praena

M. Sabaté-Gilarte, J. M. Quesada, I. Porras

And the n_TOF Collaboration



Plan of the talk.

- 1. Motivations for $^{33}\text{S}(n,\alpha)$ cross-section measurement: complete the cross-section.**
- 2. $^{33}\text{S}(n,\alpha)^{30}\text{Si}$ cross-section measurement at EAR-1: results above 10 keV.**
 - 2.1. Sample characterization.
 - 2.2. Cross section above 10 keV: resonance region.
- 3. $^{33}\text{S}(n,\alpha)$ cross-section at EAR-1 below 10 keV.**
 - 3.1 Data affected by electronic noise and background.
- 4. Optimized setup and count rate estimation at EAR-2.**

Motivations for $^{33}\text{S}(n,\alpha)^{30}\text{Si}$ measurement

- **Development of a setup for (n,α) cross-section measurements at n_TOF:**
 - (n,γ) and (n,f) up to that moment at n_TOF.
 - The setup-2012 can be used in EAR-2 and improved.
- **Astrophysics:** origin of ^{36}S , it is an open question.
- **Medical physics:** ^{33}S as cooperative target for BNCT.
- **Nuclear structure:** possible detection of excited states below 10 keV.

$^{33}\text{S}(n,\alpha)$ cross-section measurement with $^{10}\text{B}(n,\alpha)$ as reference at n_TOF EAR 1 during the campaign 2012.

$$\sigma_{33}(E_n) = \frac{C_{33}(E_n)\varepsilon_{10}(E_n)N_{10}}{C_{10}(E_n)\varepsilon_{33}(E_n)N_{33}}\sigma_{10}^{eval}(E_n)$$

Sample coating at CERN and mass determination at CNA by RBS.

Rutherford backscattering technique with alpha beam at $E_\alpha=3.7$ MeV, a good compromise between enough resolution and pure Rutherford cross-section.

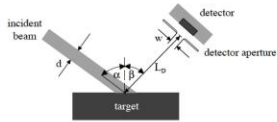
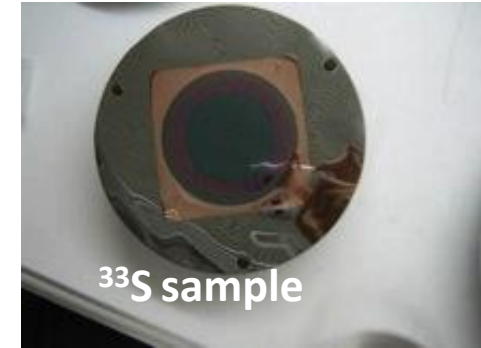


Figure 3.3: Detector geometry. d is the diameter of the incident beam, w the width of the detector aperture and L_D the distance between sample and the detector aperture. Incident angle α and exit angle β .

$$Q = N \Delta\Omega \frac{d\sigma}{d\Omega}(\bar{E}) \frac{\Delta x}{\cos \alpha}$$

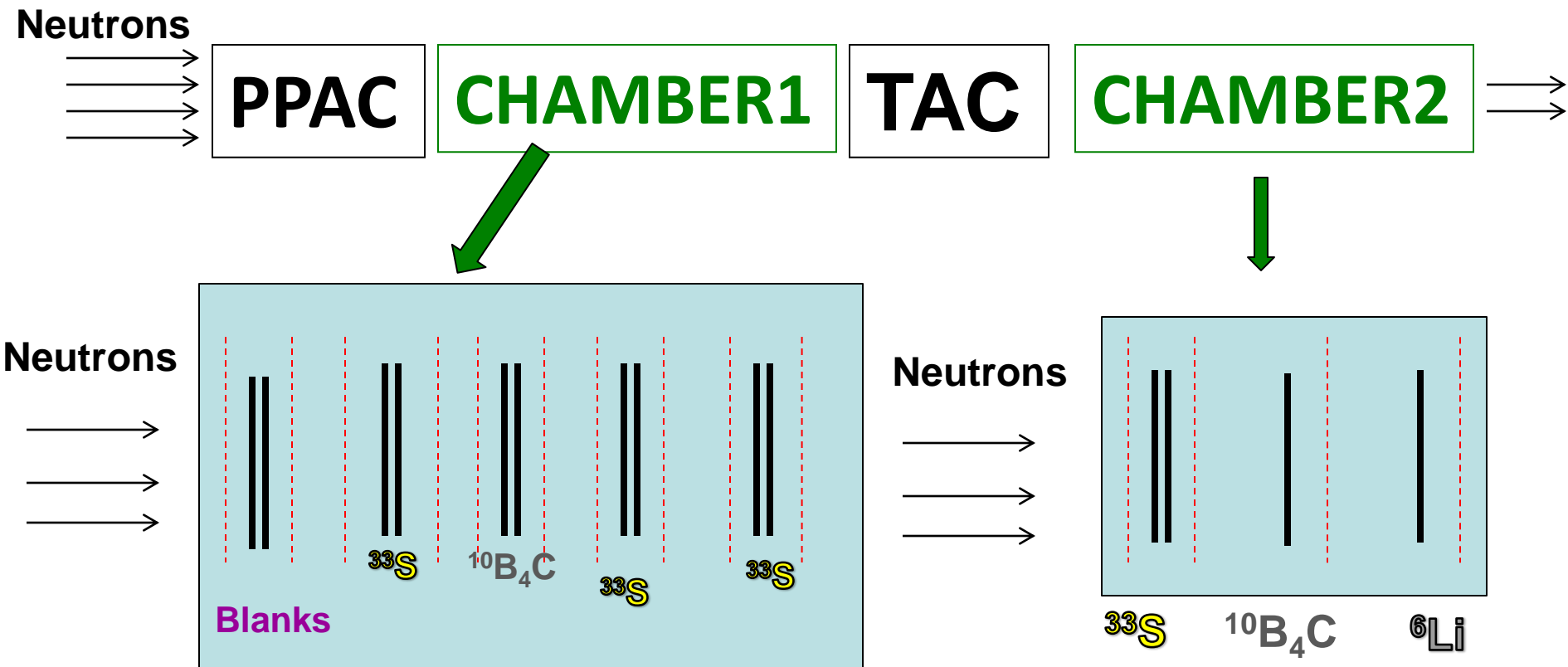


We have been able to determine the mass of the samples with an uncertainty lower than 3% thanks to the high accuracy in the determination of the number of incident alphas per stereo radian using standard references. **4% of uncertainty.**

The samples (8 cm in diameter) were scanned. Inhomogeneity lower than 3%.

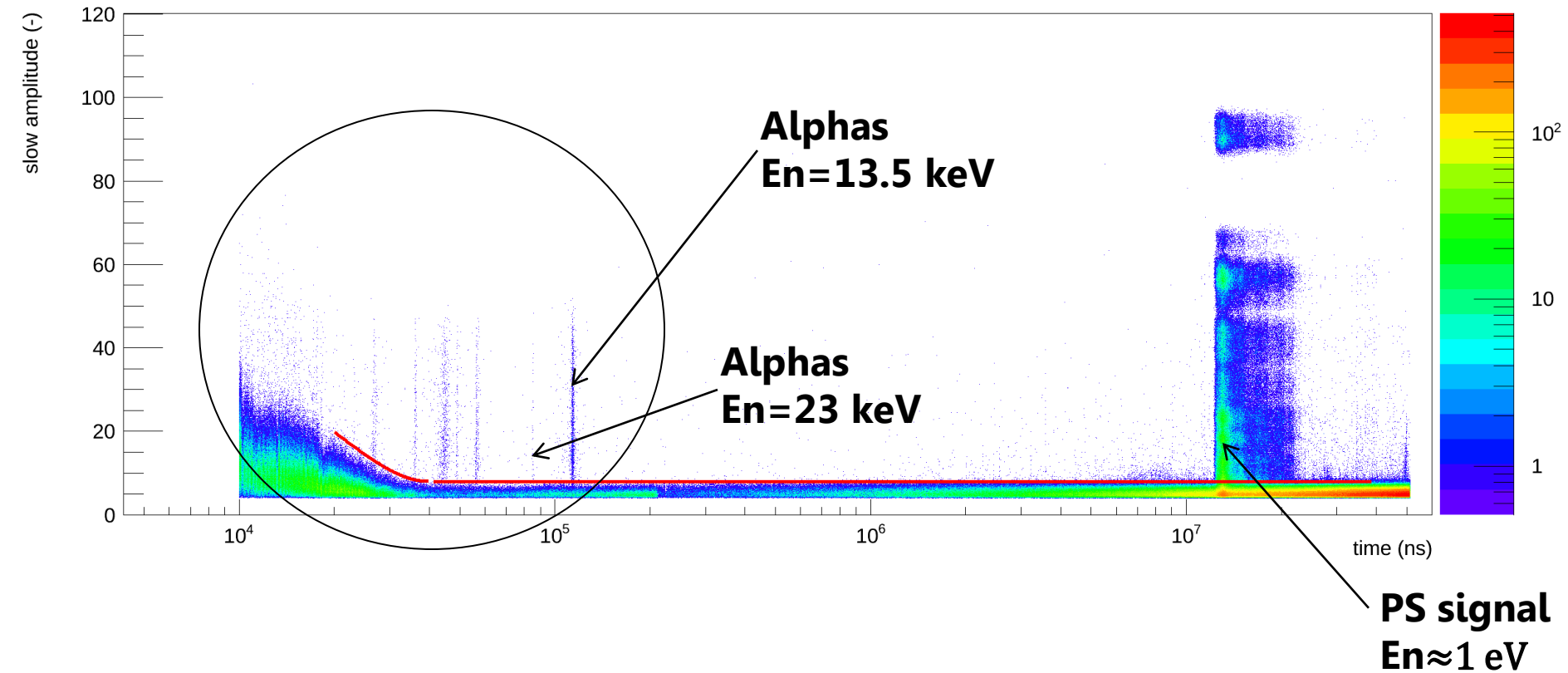
	Sample 1	Sample 2	Sample 3	Sample 4	Sample 5	Sample 6	Sample 7	Sample 8
Mass ($\cdot 10^{-7}$ at/b)	3.79 \pm 0.15	3.49 \pm 0.14	2.59 \pm 0.10	2.15 \pm 0.09	2.77 \pm 0.11	3.65 \pm 0.15	3.76 \pm 0.15	3.58 \pm 0.14

Experimental setup at n_TOF EAR1 campaign 2012.



$^{33}\text{S}(n,\alpha)$ at EAR-1: TOF & Amplitude

MGAS02_flux_h2_TA_MGAS

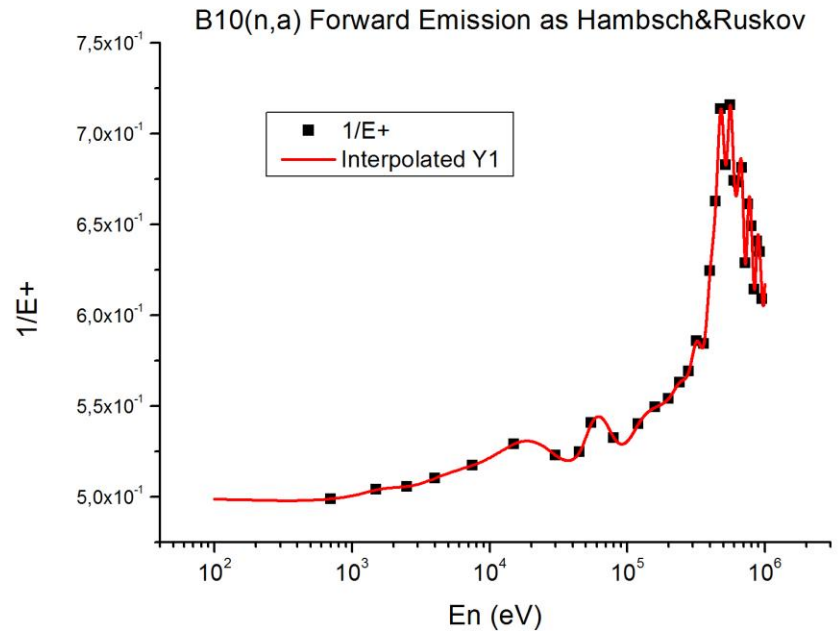
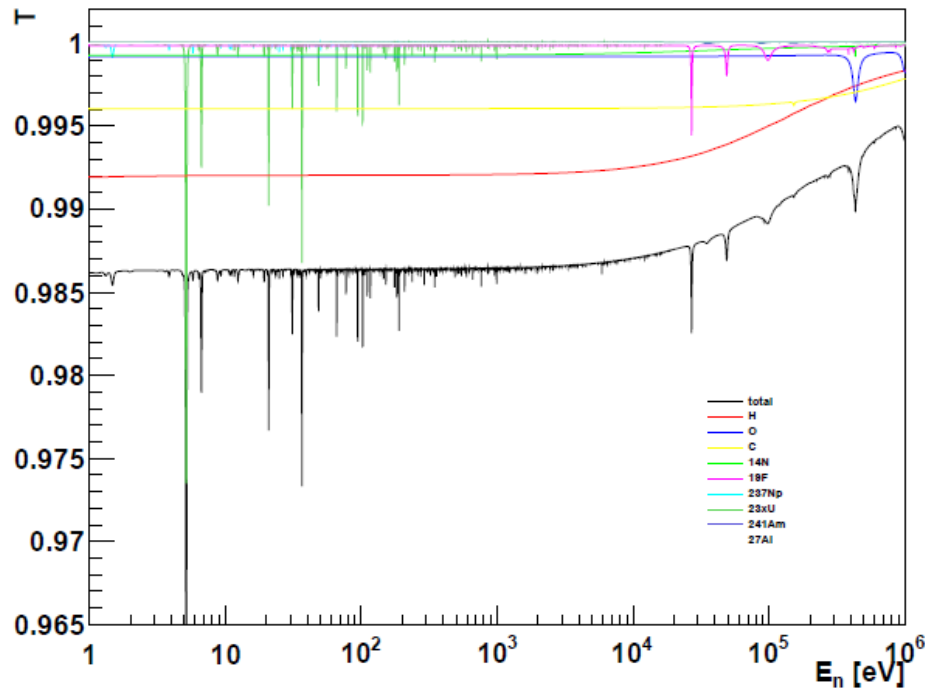


- Good discrimination of alphas from the noise-background.
- PS signal introduces a big distortion at low energies.

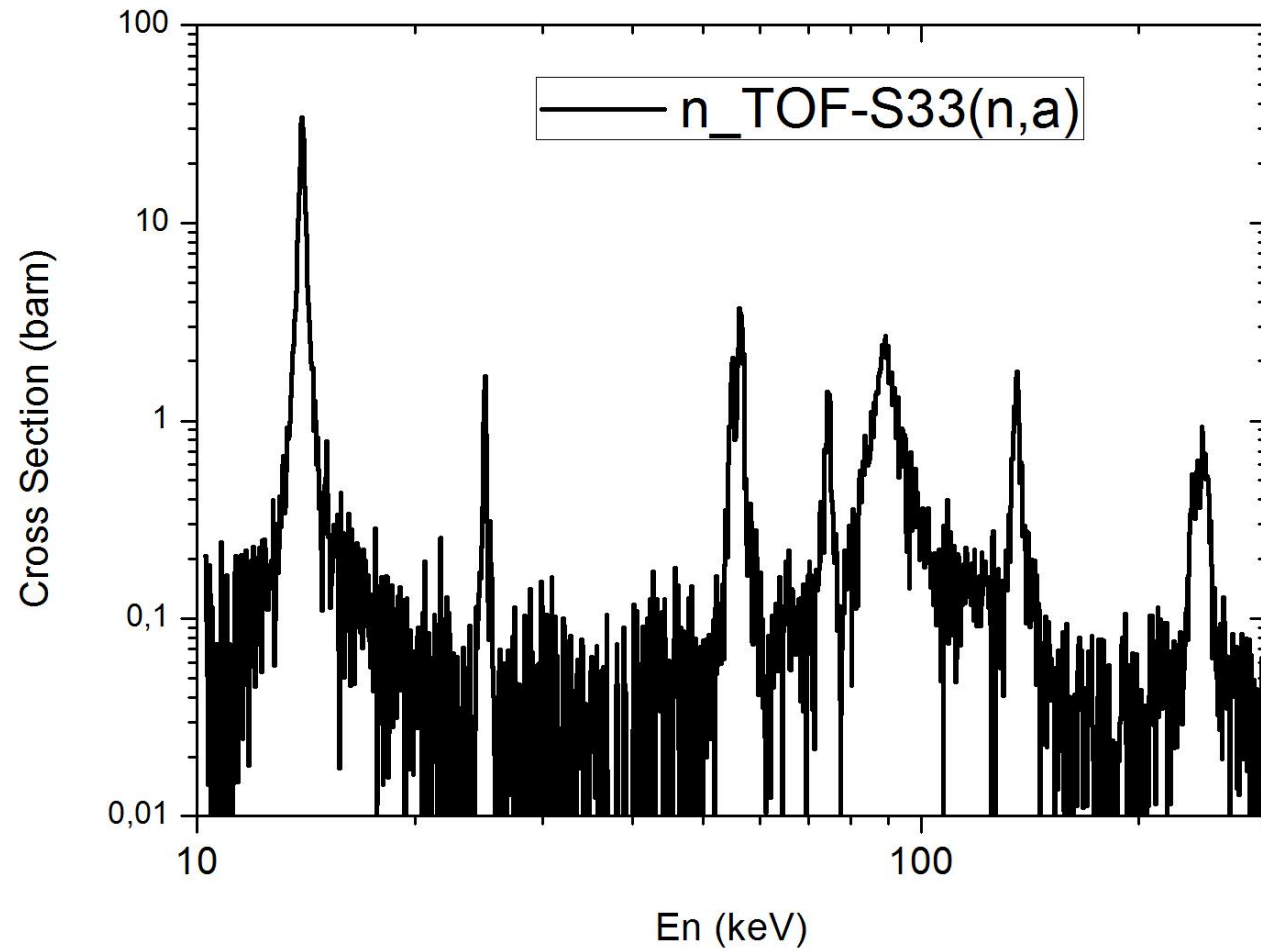
Corrections

In order to obtain the $^{33}\text{S}(n,\alpha)^{30}\text{Si}$ cross-section we correct by the transmission, angular distribution of the $^{10}\text{B}(n,\alpha)^7\text{Li}$ and CM to LAB system.

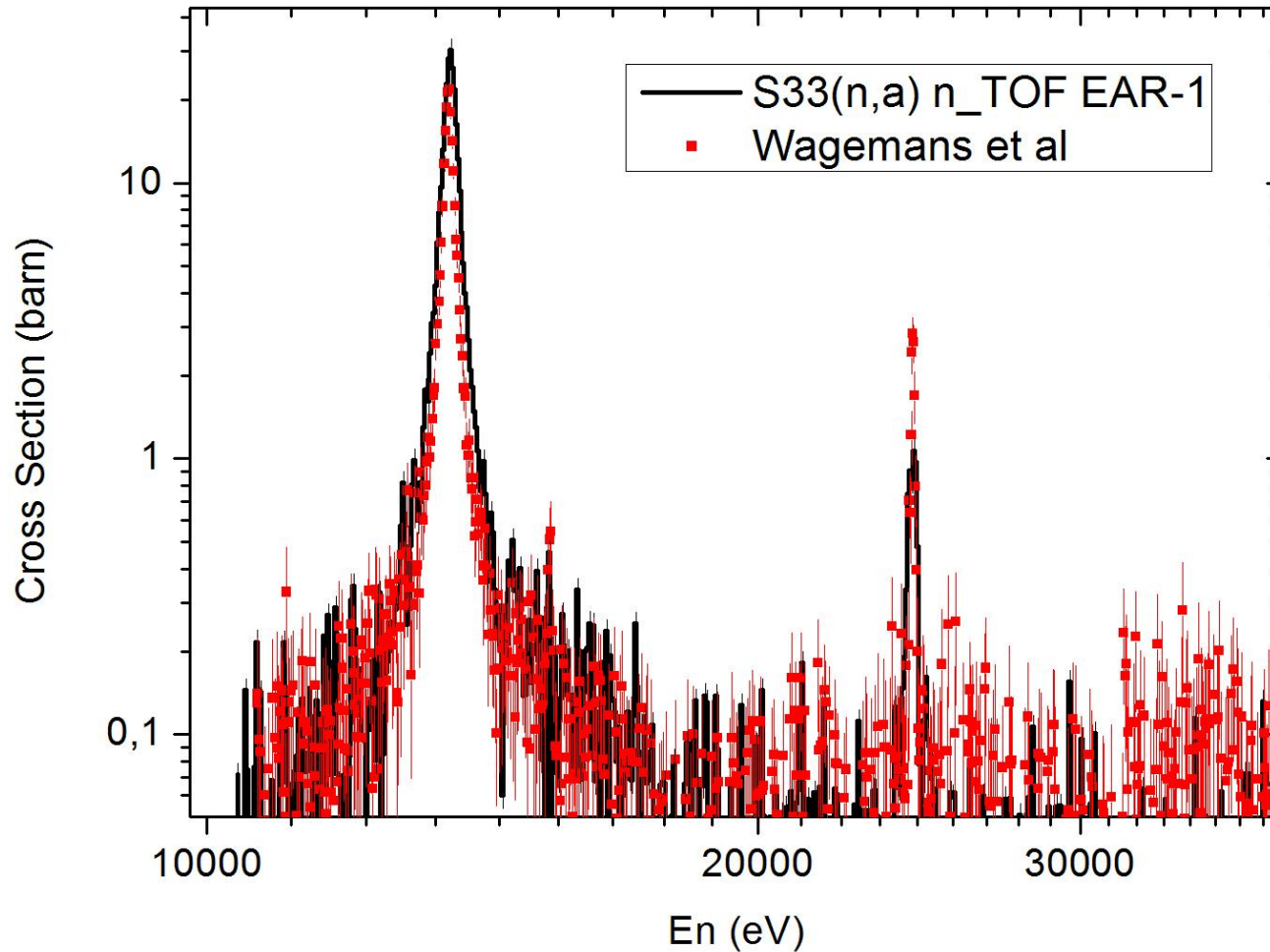
Transmission factor



$^{33}\text{S}(n,\alpha)^{30}\text{Si}$: final result, $^{10}\text{B}(n,\alpha)$ reference



$^{33}\text{S}(n,\alpha)^{30}\text{Si}$: comparison to Wagemans *et al.*



First conclusions to the experiment performed at EAR-1

- **We have developed a setup for (n,α) cross-section measurement: the setup may be improved.**
- **We have finished the characterization of the mass of the samples.**
- **We have finished the data analysis of the $^{33}\text{S}(n,\alpha)$ cross-section resolving the resonance region from 10 to 300 keV.**
- **We have found an agreement with Wagemans *et al.* with differences for few resonances.**
- **The main objectives of the proposal at EAR-1 have been achieved.**

$^{33}\text{S}(n,\alpha)$ status below 10 keV: motivation for EAR-2

Status of $^{33}\text{S}(n,\alpha)^{30}\text{Si}$ experimental data.

- Auchampaugh *et al* PRC 12 1126–33 1975: (n, γ) and (n, α) from 10 to 700 keV. TOF.
- Wagemans *et al* NPA 469 497–506 , 1987: (n, α) from 10 keV to 1 MeV. TOF.
- Coddens *et al* NPA 469 480–96 , 1987: (n,tot) from 10 keV to 2 MeV. TOF.

Wagemans *et al*

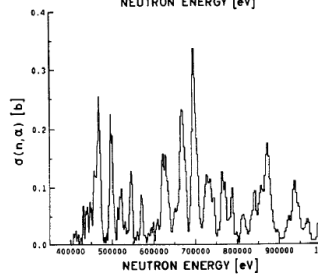
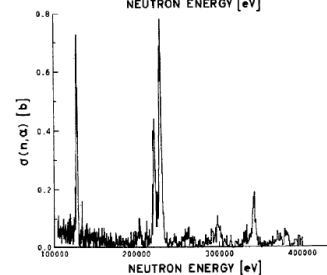
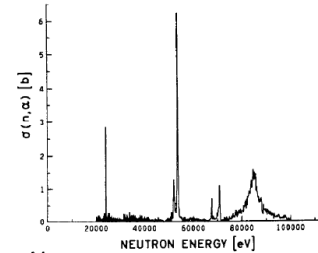
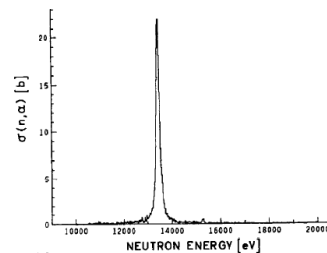
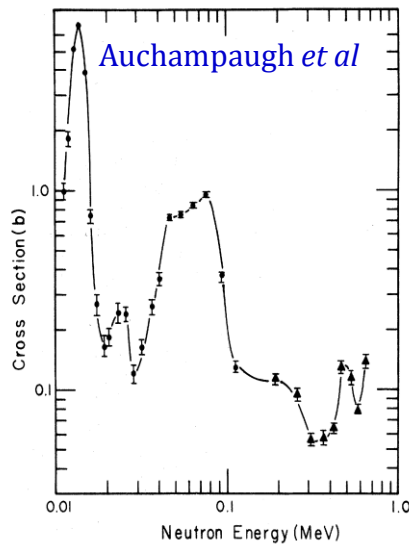
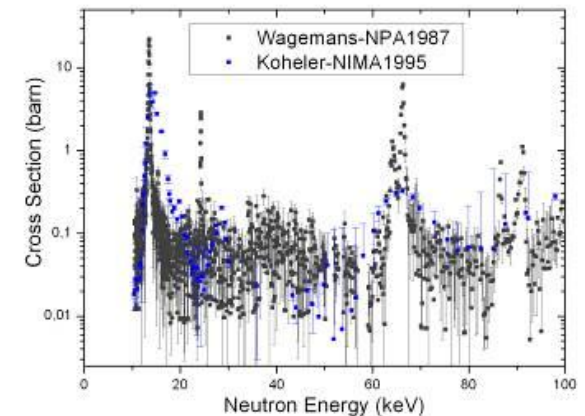
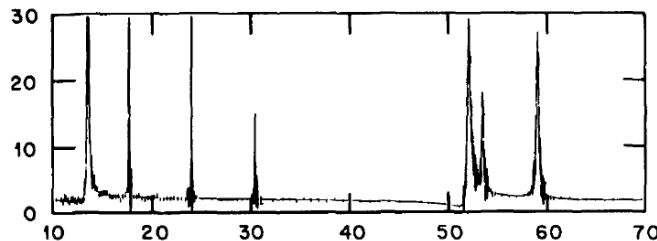


Fig. 2. The measured $^{33}\text{S}(n,\alpha)$ cross section between 10 keV and 1 MeV neutron energy.



Coddens *et al* (TRANSMISSION)

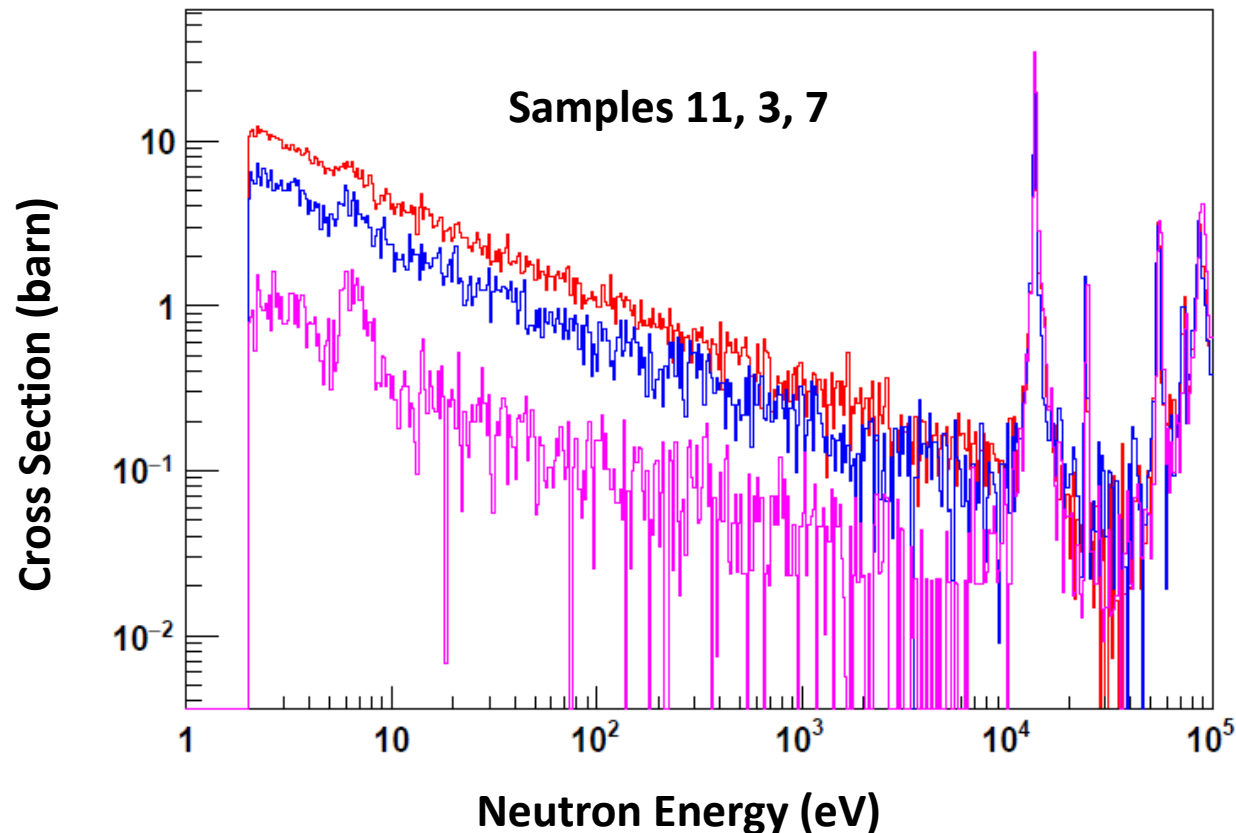


- No data below 10 keV.
- At thermal discrepancies of a factor 4.

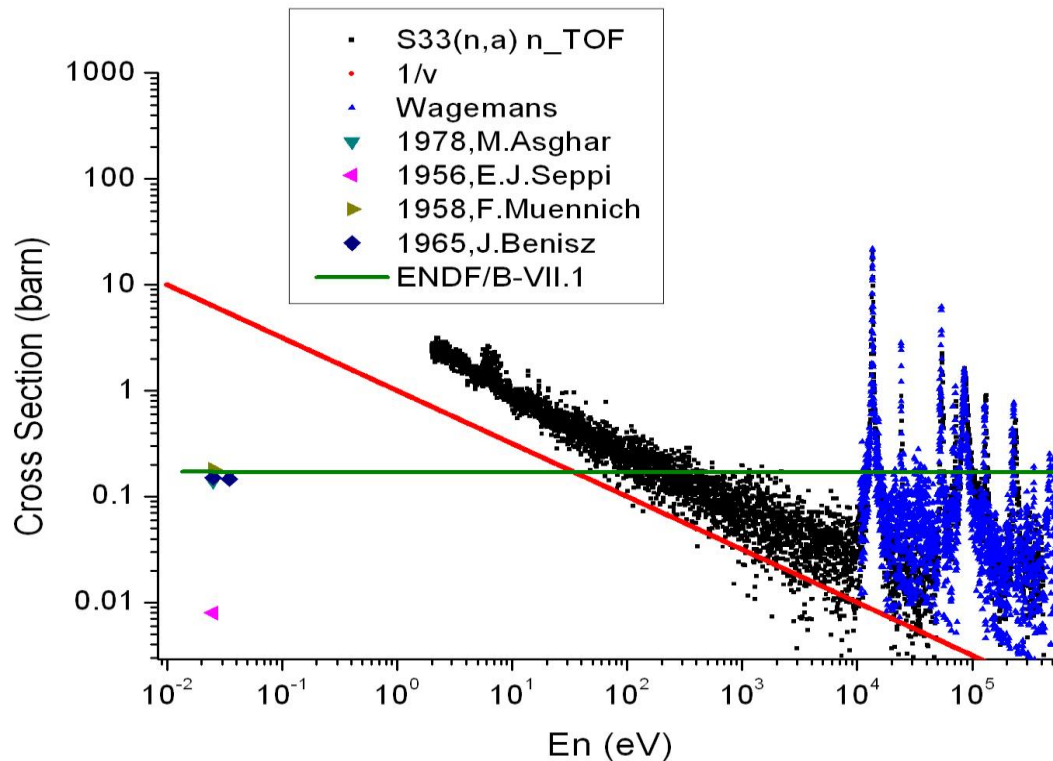
$^{33}\text{S}(n,\alpha)^{30}\text{Si}$ at EAR-1: data below 10 keV?

Figure shows the cross-section obtained with 3 different samples during the experiment at EAR-1.

It can be noticed the agreement in the resonance region meanwhile below 10 keV the discrepancies are evident.



$^{33}\text{S}(n,\alpha)^{30}\text{Si}$ at EAR-1: thermal comparison.



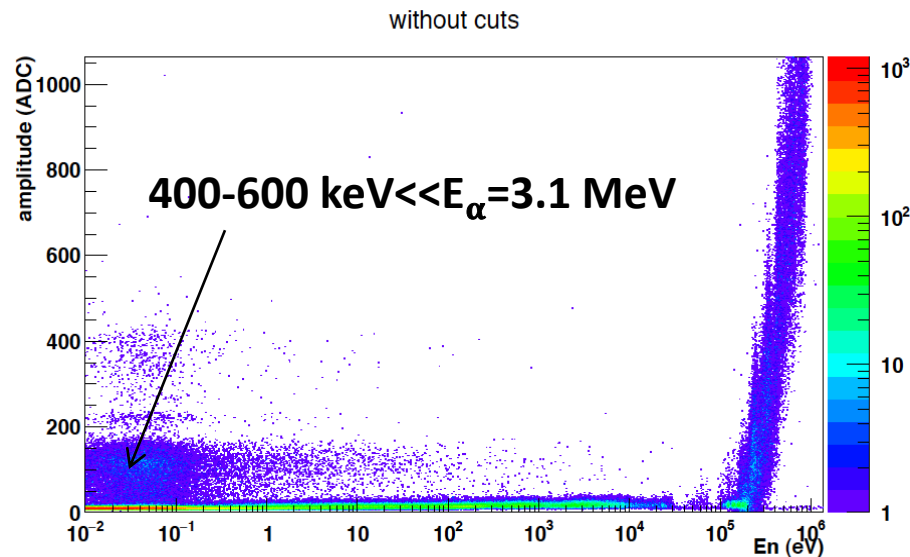
The extrapolation of our data ($1/v$) to thermal energy provides a value two order of magnitude higher than experimental available data at thermal point.

This could be an indication that our data may be affected of noise and no adequate background subtraction at energies below 10 keV.

Setup and count rate estimation at EAR-2

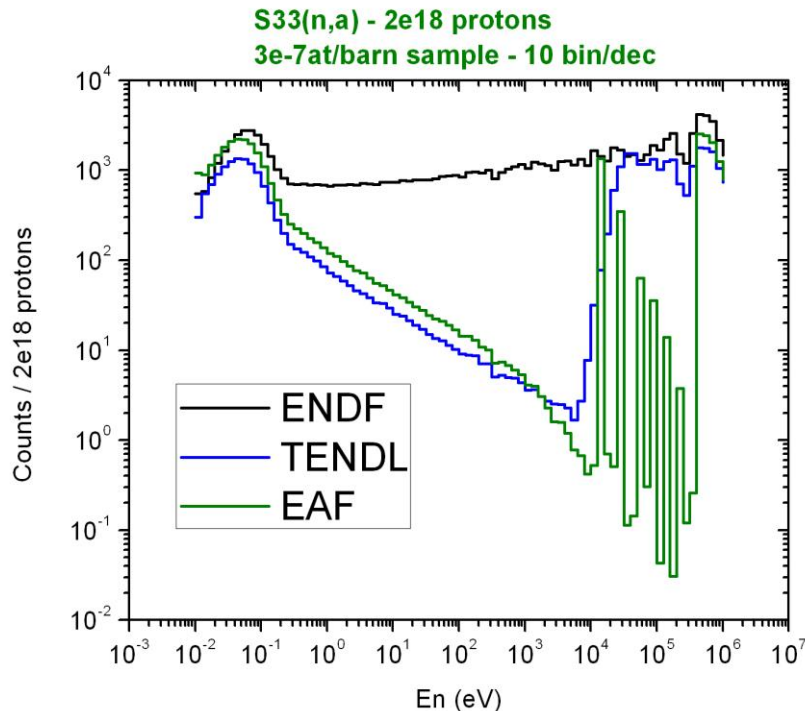
Test at EAR-2: improvements on the EAR-1 setup.

- ❑ The higher flux available at EAR-2 will allow a **higher signal-to-background ratio**.
- ❑ The improvements performed as a better grounded at EAR-2, better shielding in the new Micromegas preamplifier will allow a low electronic noise ambient.
- ❑ In addition to this, there is **no PS signal** affecting our data at low energy as shown in the figure (Neutron Energy & Amplitude at EAR-2).
- ❑ Figure shows a preliminary test with Micromegas detector calibration for sample backing characterization at EAR-2.
- ❑ Signals will be well above the noise and background at EAR-2.



$^{33}\text{S}(n,\alpha)^{30}\text{Si}$ count rate at EAR-2 for $2e18$

- ❑ Because our data below 10 keV may be affected by electronic noise and background we use 3 existing evaluations that provided the largest and lowest value of the $^{33}\text{S}(n,\alpha)$ cross-section. Neutron flux at EAR-2 and $3e-7$ at/b sample.
- ❑ ICRU recommends that radiation dose delivered should be within 5% of the prescribed dose that means <5% uncertainty at each step.



$2 \cdot 10^{18}$ protons may allow to have less than 5% statistical uncertainty with a lower energy resolution than at EAR-1 (10bpd). Resonances may be resolved although with lower energy resolution (EAF evaluation).

Summary of $^{33}\text{S}(n,\alpha)$ proposal at n_TOF-EAR2

- We have ready a setup for (n, α) cross-section measurement at n_TOF
- $^{33}\text{S}(n,\alpha)/^{10}\text{B}(n,\alpha)$ at EAR-1 was measured in 2012 and we have finished the data analysis extracting the cross-section above 10 keV and resolving the resonances.
- We have collected data below 10 keV that can be affected by residual electronic noise, and a non-optimized signal-to-background ratio. Extrapolation at thermal energy is an indication.

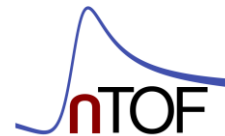
- We worked in a new electronics and optimized setup at EAR-2 for Micromegas.
- We propose to measure the $^{33}\text{S}(n,\alpha)$ at EAR-2 to complete the cross-section with motivations in nuclear astrophysics, medical physics and nuclear structure.
- **The background and noise will be characterized for each ^{33}S -detector (2), blank-detector and empty-detector.**
- **We request $2e18$ protons.**
- **We could run in parasitic.**

Thank you

Javier Praena

M. Sabaté-Gilarte, J. M. Quesada, I. Porras

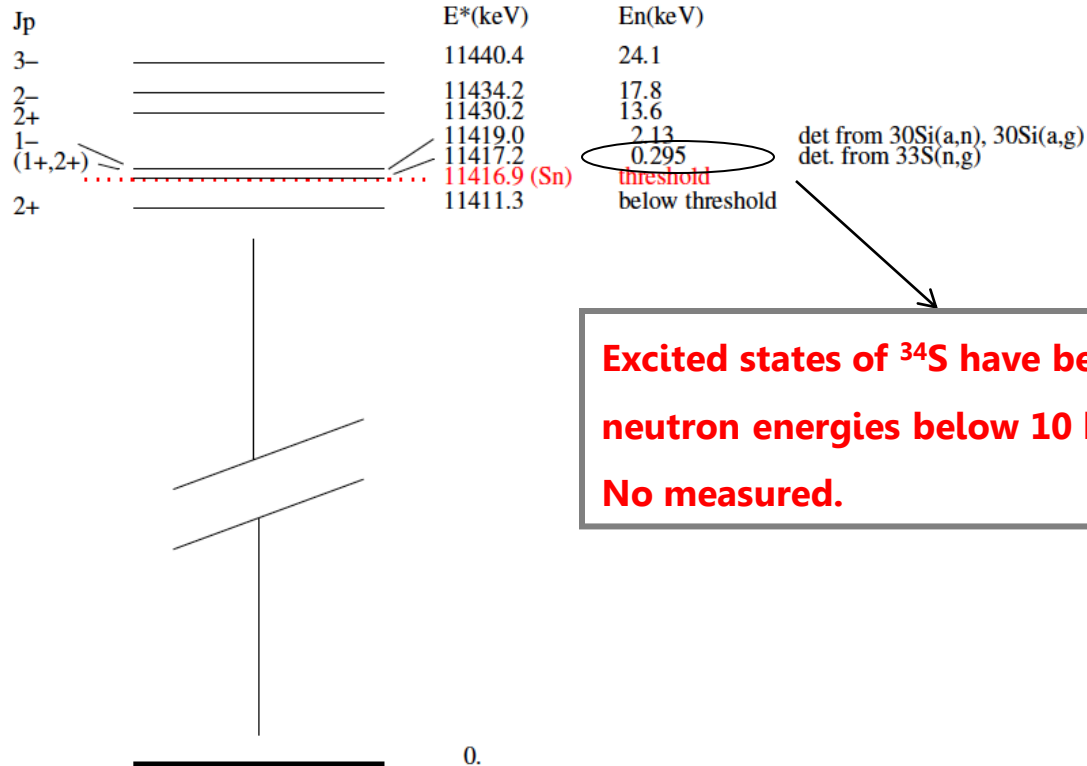
And the n_TOF Collaboration



Nuclear structure of the ^{34}S : states below 10 keV.

Excited states of ^{34}S near neutron separation energy

N. Nica and B. Singh, Nucl. Data Sheets 113, 1563–1733 (2012)



**Excited states of ^{34}S have been predicted for neutron energies below 10 keV of the $^{33}\text{S}(n, \alpha)$.
No measured.**

The major part of the levels were measured by Wiecher *et al.* NP A92 (1967) 175-192 with inverse kinematics experiments: $^{30}\text{Si}(\alpha, n)^{33}\text{S}$ and $^{30}\text{Si}(\alpha, \gamma)^{34}\text{S}$.

Moreover, anisotropy angular emission was measured with the inverse kinematic reaction and it may be related to alpha-cluster formation and non-compound nucleus effect.



Motivations: ^{36}S nucleosynthesis

Ar34 844.5 MS	Ar35 1.775 S	Ar36 0.336 S	Ar37 35.04 D	Ar38 0.0632	Ar39 269 Y
Cl33 2.511 S	Cl34 1.8264 S	Cl35 75.77	Cl36 30.000 Y	Cl37 24.23	Cl38 37.24 M
S32 95.02	S33 0.75	S34 4.21	S35 87.38 D	S36 0.02	S37 5.05 M
P31 100	P32 4.262 D	P33 25.34 D	P34 12.43 S	P35 47.3 S	P36 5.6 S
Si30 3.087	Si31 1.573	(n,α)	Si33 32 S	Si34 2.77 S	Si35 0.78 S
Al29 6.56 M	Al30 3.60 S	Al31 644 MS	Al32 33 MS	Al33 >1 US	Al34 60 MS

$^{33}\text{S}(n,\alpha)$	MACS, $kT=30$ keV
Auchampaugh <i>et al</i> PRC 12 1126 (1975)	(690±170) mb TOF
Wagemans <i>et al</i> NPA 469 497 (1987)	(227±20) mb TOF
Schatz <i>et al</i> PRC 51 379 (1995)	181 mb (175±9) mb Activation
Woosley <i>et al</i> At. D. Nucl. D. Tab. 22 371 (1978)	224 mb Model

ENDF/B-VII.1, USA 2011

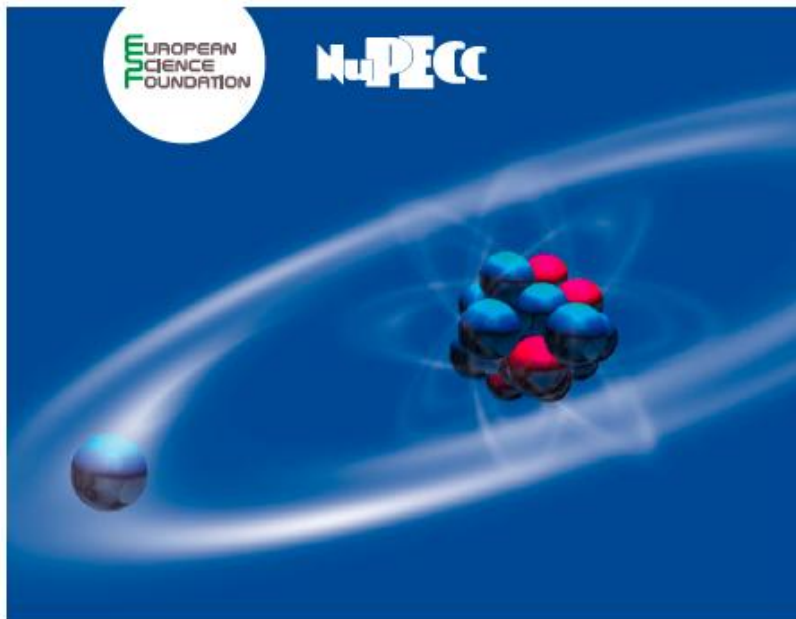
(n,α)

30

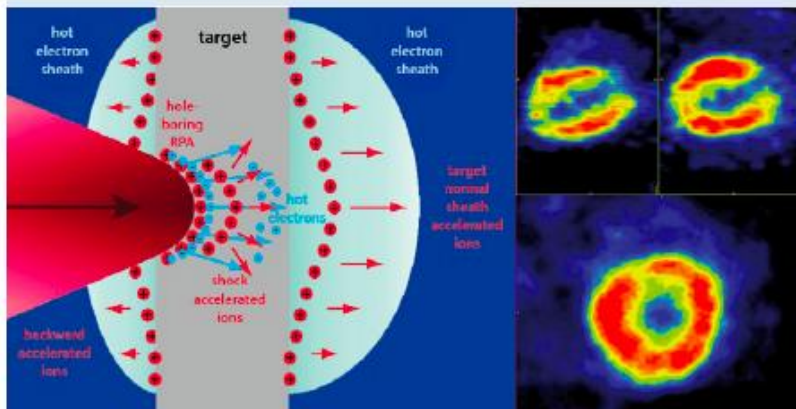
1.903E2

- Reifarth *et al* [Astro. J. 528:573-581 (2000)] obtained the MACS of $^{34}\text{S}(n,\gamma)$ by the activation technique showing that ^{34}S could act as bottle-neck in this path.
- The origin of ^{36}S remains an open question.
- **How did the authors calculate the MACS using the provided cross-section by TOF?**
- **What was the cross-section behavior below 10 keV? Notice $E_n < 10$ keV is main contribution to the cross-section for a Maxwellians $kT=30$ keV.**
- **In addition to this, the activation measurement, Schatz et al, used quasi maxwellian spectrum at 25 keV generated by the $\text{Li7}(p,n)$ reaction. For the correction of the spectrum and for the extrapolation to 30 keV the assumption of the cross-section is mandatory.**
- **All authors claimed problems with the sample coating. Our RBS studies throughout 3 years have demonstrated the stability of our samples.**

Boron Neutron Capture Therapy



Nuclear Physics European Collaboration Committee (NuPECC)
Nuclear Physics for Medicine

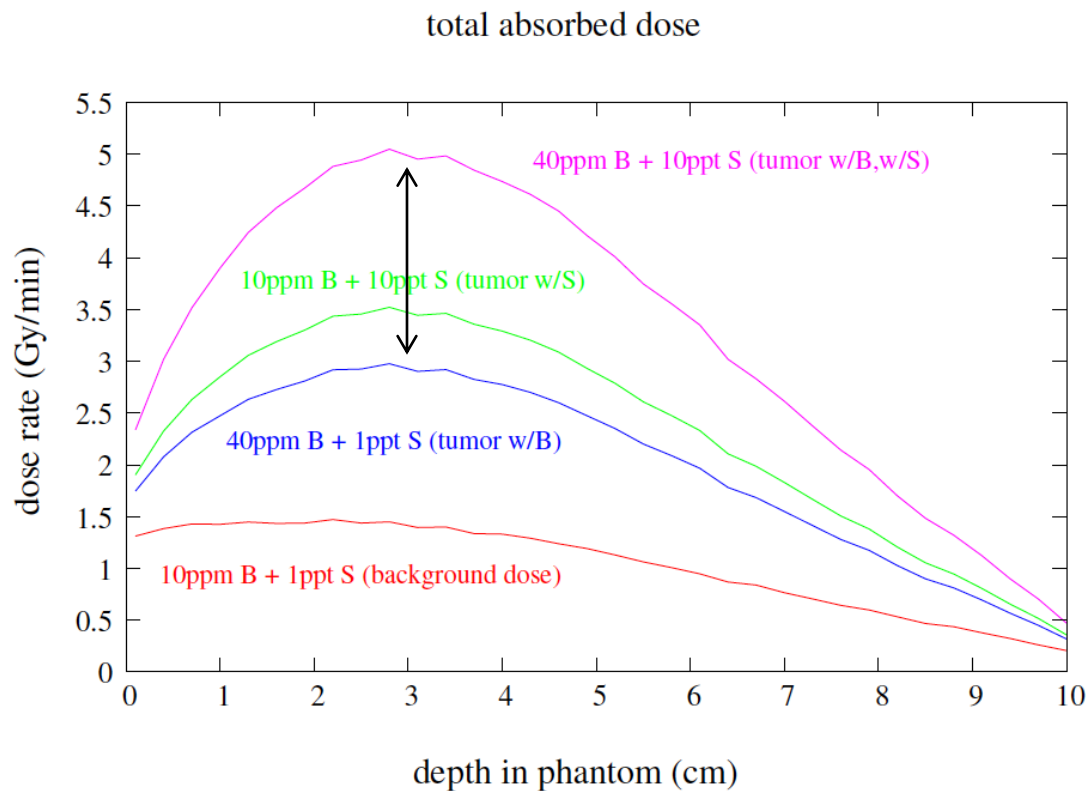


Chapter I Hadrontherapy

Conveners: Marco Durante (GSI) – Sydney Galès (Orsay, FAIR, ELI)

1. Introduction			11
2. Facilities in operation and planned			14
2.1 Historical development of hadron radiotherapy facilities	14	2.2 Proton and carbon ion facilities in operation	15
		2.3 Future facilities	15
3. Accelerators			18
3.1 Introduction	18	3.5 Cyclotrons and synchrotrons: advantages and disadvantages	21
3.2 Historical development	18	3.6 Current status	22
3.3 Microbeams	19	3.7 Future	22
3.4 Beam features for a hadrontherapy centre	19		
4. Beam delivery			24
4.1 Principle and interfacing	24	4.5 Beam delivery performances	26
4.2 From the accelerator to the treatment rooms	24	4.6 Other considerations	26
4.3 Beamline orientation in the treatment rooms	24	4.7 Perspectives and challenges	26
4.4 Beam delivery methods	25		
5. Dosimetry			27
5.1 Introduction	27	5.3 R&D	28
5.2 Dosimetry tools for hadron radiotherapy	27		
6. Moving targets			30
6.1 Introduction	30	6.4 Motion mitigation strategies	31
6.2 Imaging moving organs	30	6.5 Summary	32
6.3 Motion detection	31		
7. Radiology			33
7.1 Introduction	33	7.4 Hypofractionation	35
7.2 RBE	33	7.5 Combined therapies	35
7.3 Cancer stem cells	34		
8. Modelling			37
8.1 Introduction	37	8.4 Fragmentation	39
8.2 Monte Carlo modelling in hadrontherapy	37	8.5 Simulations of PET images	39
8.3 Secondary neutrons	38	8.6 Summary	40
9. Treatment planning			41
9.1 Introduction	41	9.3 Quality assurance aspects	44
9.2 The treatment planning process	41	9.4 Current developments	44
10. Boron neutron capture therapy			46
10.1 Introduction	46	10.4 Accelerator-based neutron sources	48
10.2 BNCT in clinical practice	46	10.5 Therapeutic neutron beams	50
10.3 BNCT physics	48	10.6 Conclusions	52
11. Clinical programme update in particle therapy			53
11.1 Introduction	53	11.3 Development of carbon ions indications	54
11.2 Proton therapy indications	53	11.4 Perspectives	54
12. Outlook			56

^{33}S in AB-NCT: dose rate B-10&S-33 for a neutron beam of 10 keV, therefore no resonance contribution

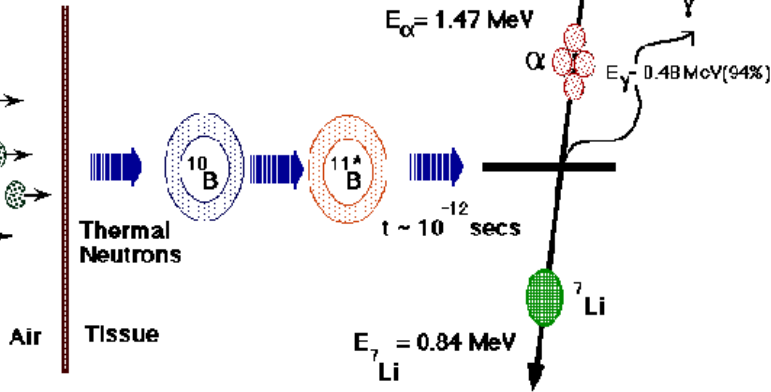


The enhancement of the dose due to the presence of S-33 is very important allowing a lower neutron flux, deeper tumours, and/or shorter time treatment

Clinical BNCT: the past is nuclear reactors.

Incident Epithermal

Neutrons



cells. Two drugs are nowadays available for clinical investigations: BSH (*mercaptoundecahydro-closo-dodecaborate* $\text{Na}_2^{10}\text{B}_{12}\text{H}_{11}\text{SH}$) and BPA (*para-borophenylalanine* $\text{C}_9\text{H}_{12}^{10}\text{BNO}_4$). Other

^{10}B is the isotope widely used for this purpose, being accumulated selectively into tumour cells by several mechanisms. For example, borophenylalanine (BPA) is selectively and preferentially accumulated into tumour cells via the augmented metabolism of amino acids in comparison to normal cells. The first

Since 1994, at least 227 patients with glioblastoma multiforme, a form of brain cancer associated with a poor prognosis, have undergone BNCT, in many cases in combination with chemotherapy (such as Bevacizumab or Temozolamide or with external beam radiotherapy, EBRT). The inclusion of BNCT in the therapeutic scheme produced a significant increase of the overall survival rate after 30 months from diagnosis (0% vs. 20% in no-BNCT vs. BNCT group and 0% in no-BCNT vs. 30% in BNCT+EBRT group). Moreover, from 1999, about 165 patients with head and neck cancer were treated by BNCT with a recognised effect from a clinical point of view (reduction of morbidity) and a recovery in overall survival of 38% after 24 months from the date of diagnosis.

Table 10.1. Operative BNCT centres

Centre	States	Neutron source	Neoplasm	N° of treated patients*
Helsinki University Central Hospital, Helsinki, Finland	Europe	FIR-1, VTT Technical Research Centre, Espoo	GB and HN	50 GM 2 AA 31 HN
University of Tsukuba, Tsukuba City, Ibaraki	Japan	JRR-4, Japan Atomic Energy Agency, Tokai, Ibaraki	GB	20 GM 4 AA
University of Tokushima, Tokushima	Japan	JRR-4 (Kyoto University Research Reactor, Osaka)	GB	23
Osaka Medical College and Kyoto University Research Reactor, Kyoto University, Osaka and Kawasaki Medical School, Kurashiki	Japan	KURR	GB, HN, CM	30 GBM 3 AA 7 Men 124 HN
Taipei Veterans General Hospital, Taipei, Taiwan	Republic of China	THOR, National Tsing Hua University, Hsinchu, Taiwan	HN	10
Instituto de Oncología Angel H, Buenos Aires	Argentina	Barieloche Atomic Center	CM and AT	7CM 3 AT

* GM: glioblastoma multiforme; CM: cutaneous melanoma; AA: anaplastic astrocytoma; HN: head and neck cancer; Men: meningioma; AT: anaplastic thyroid cancer

Clinical BNCT: nuclear reactor results.

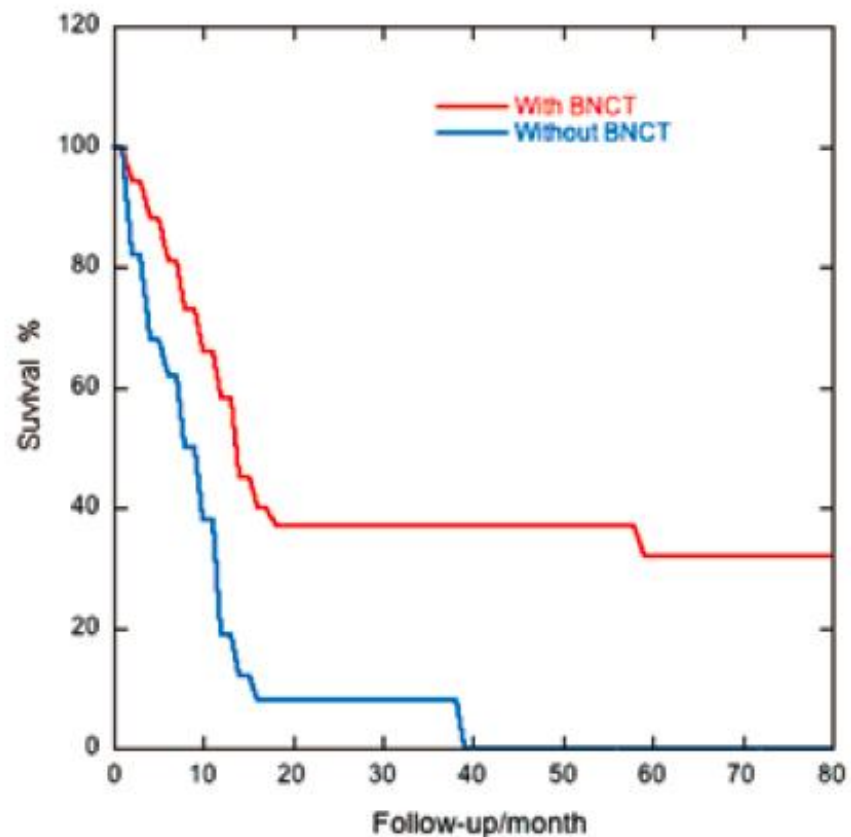
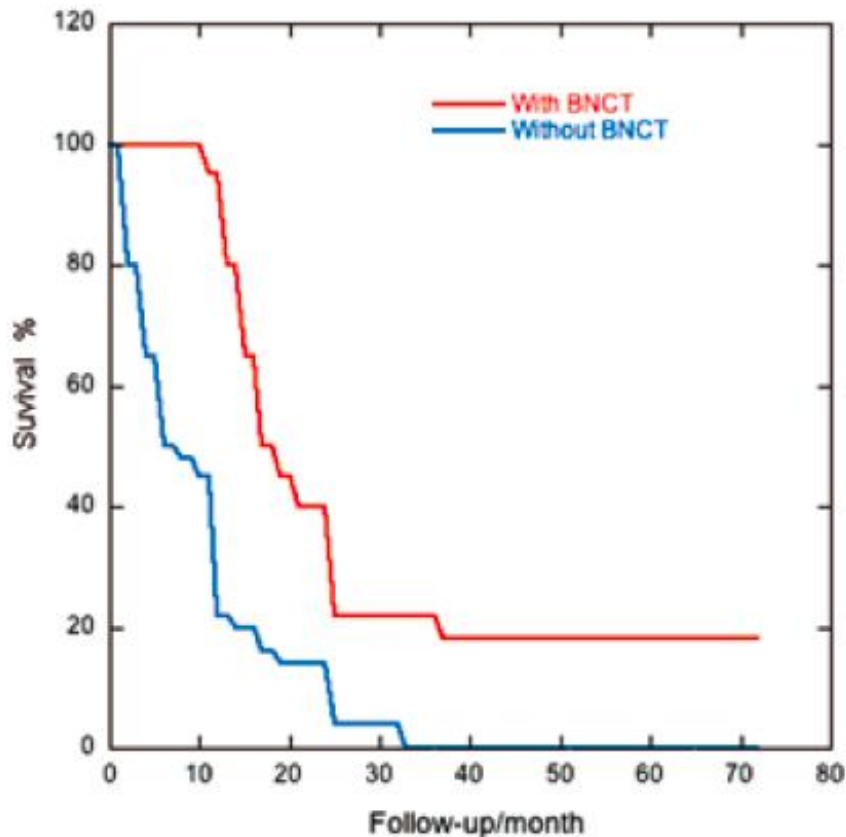
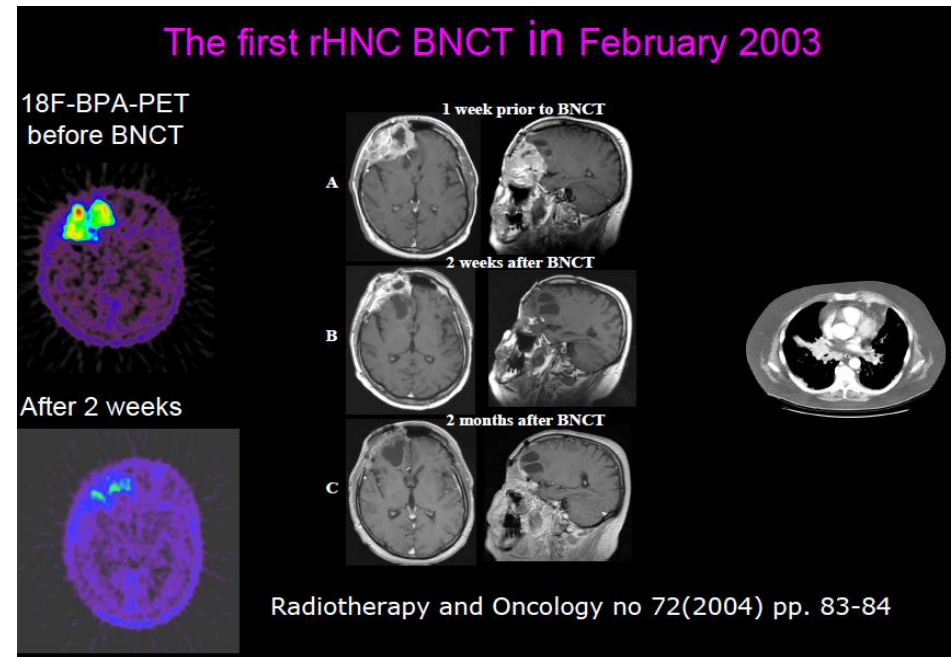
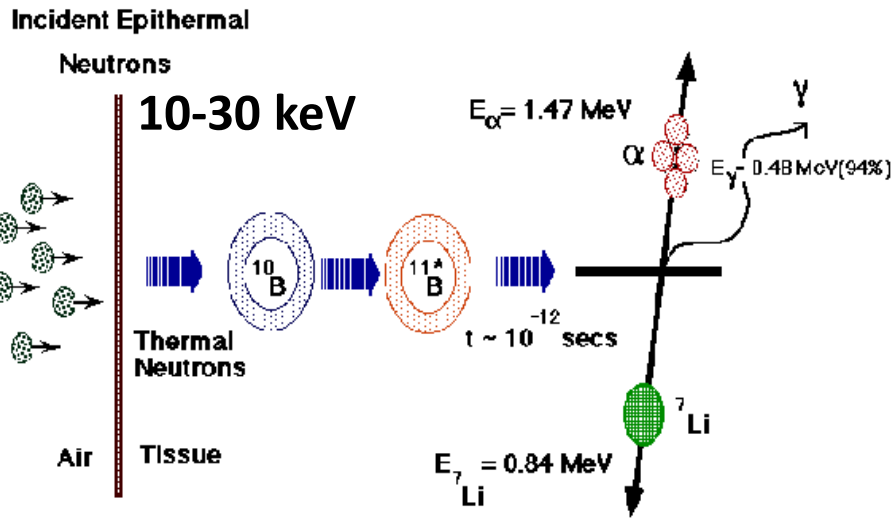


Figure 10.2. Left side, Kaplan–Meier plot of the overall survival for all newly diagnosed glioblastoma treated and not treated with BNCT [from Kawabata *et al.* (2009). Survival benefit from boron neutron capture therapy for the newly diagnosed glioblastoma patients. *Appl. Radiat. Isot.* **67**: S15-18]. Right side, Kaplan–Meier survival plots of patients with recurrent head and neck cancer treated with and without BNCT [from Kato *et al.* (2009). Effectiveness of boron neutron capture therapy for recurrent head and neck malignancies. *Appl. Radiat. Isot.* **67**: S37-42].

Motivations: ^{33}S as cooperative target in NCT



- Past: thermal neutron beams from nuclear reactor.
- Future: epithermal neutron beams from accelerator-based neutron source.
- Neutron production, $\text{Li}(p,n)$, solid and liquid lithium targets, high current low energy accelerators such RFQ and new IBA electrostatic accelerators, nanotechnology for boron carriers, dosimetry studies, treatment planning.
- Experimental treatments. Finland. <http://clinicaltrials.gov/show/NCT00114790>

Clinical BNCT: the present/future is accelerators.

- Epithermal (around 10 keV) neutron beams are the more adequate to have enough penetration in the body but 2-3 centimeters of tissue for moderation are necessary for $^{10}\text{B}(n,\alpha)$ reaction, a lot of neutrons are lost (origin of the S-33 idea).
- At present the neutron beam shaping must be based on the IAEA figure of merit for shallow and deep tumours even the “new” AB-BNCT, it should change very soon.

thermal ($E_n < 0.5\text{eV}$), epithermal ($0.5\text{eV} < E_n < 10\text{keV}$) and fast ($E_n > 10\text{keV}$) neutrons, IAEA recommends the following fluence rates and absorbed dose rates for shallow and deep tumours.

Shallow tumours

$$\Phi_{\text{th}} \geq 10^9 \text{ cm}^{-2}\text{s}^{-1}$$

$$\Phi_{\text{th}} / \Phi_{\text{tot}} \geq 0.9$$

$$\dot{D}_{\text{n(epi+fast)}} / \Phi_{\text{th}} \leq 2 \times 10^{-3} \text{ Gy cm}^2$$

$$\dot{D}_{\gamma} / \Phi_{\text{th}} \leq 2 \times 10^{-3} \text{ Gy cm}^2$$

Deep tumours

$$\Phi_{\text{epi}} \geq 10^9 \text{ cm}^{-2}\text{s}^{-1}$$

$$\Phi_{\text{epi}} / \Phi_{\text{th}} \geq 100; \quad \Phi_{\text{epi}} / \Phi_{\text{fast}} \geq 20$$

$$\dot{D}_{\text{n(fast)}} / \Phi_{\text{epi}} \leq 2 \times 10^{-3} \text{ Gy cm}^2$$

$$\dot{D}_{\gamma} / \Phi_{\text{epi}} \leq 2 \times 10^{-3} \text{ Gy cm}^2$$

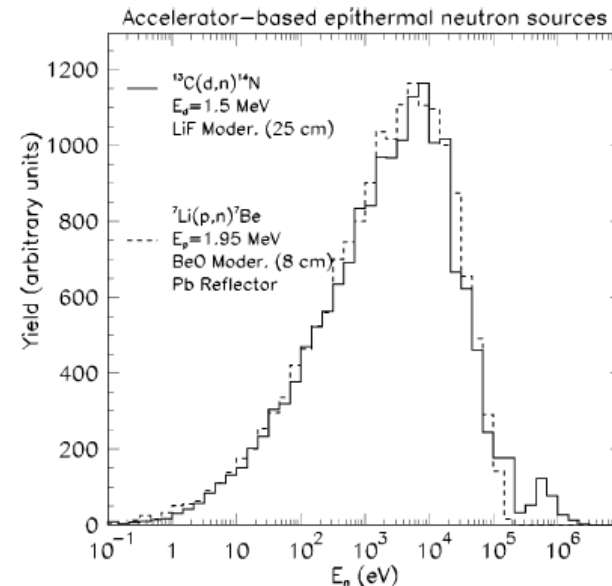
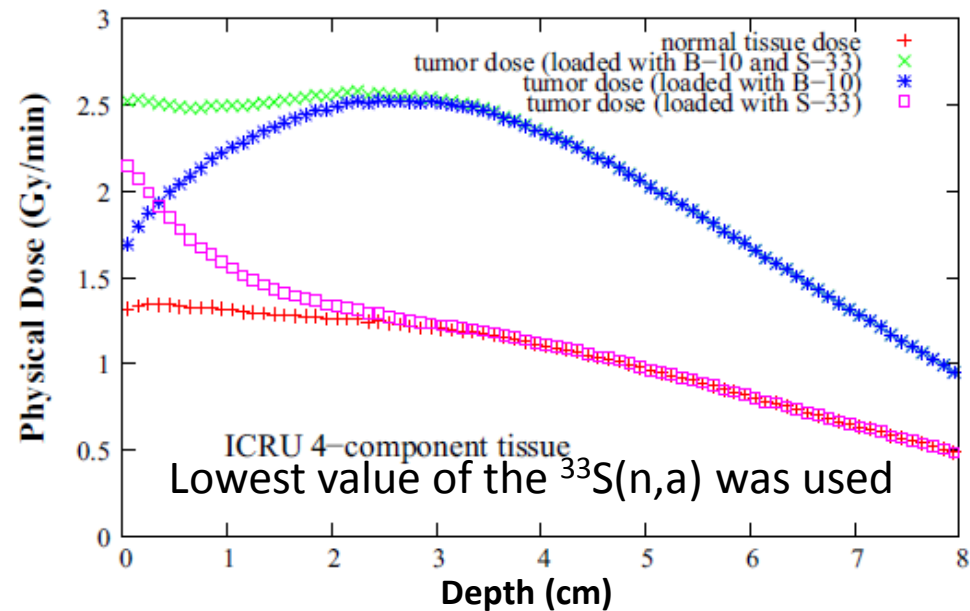
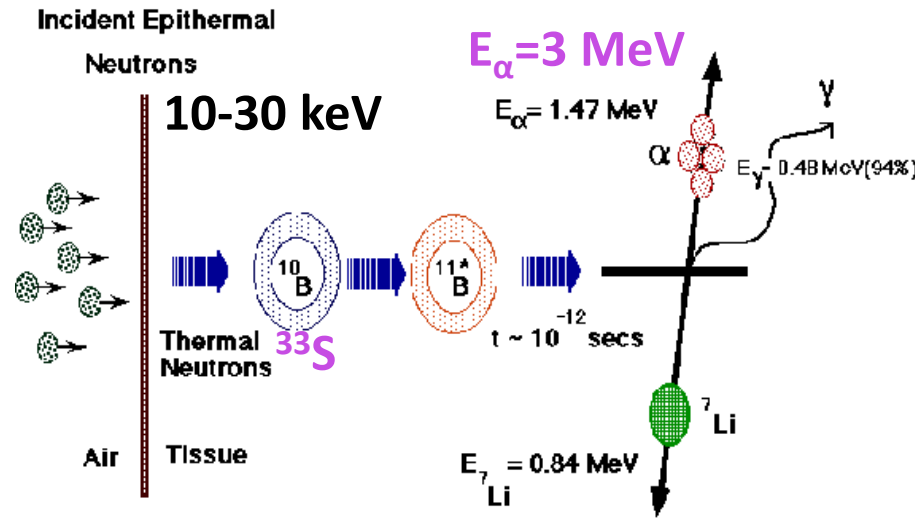


Fig. 3. Epithermal neutron energy spectra produced with the $^{13}\text{C}(d,n)^{14}\text{N}$ and the near-threshold $^7\text{Li}(p,n)^7\text{Be}$ reactions. The optimal beam shaping assembly used for each reaction is indicated.

Motivations: ^{33}S as cooperative target in NCT



- S-33 concentration of the order of mg/g based on the addition of cystine to the culture medium, as *PW Gout et al.*, *Increased cystine uptake capability associated with malignant progression of Nb2 lymphoma cells, Leukemia 11, 1329–1337 (1997)*. Selectivity *Coderre et al.*, *J. Nucl. Med. 27, 1157 (1986)*.
- The presence ^{33}S enhances the dose in the first centimetres in tissue: motivation EAR-1.
- For instance, NECK-HEAD tumours grow to the skin so S-33 may be very useful. Also tumours as lung tumours have not a treatment solution, therefore S-BNCT may be an interesting research line.

* I. Porras *Phys. Med. Biol.* 53 (2008), J. Praena *et al.*, *ARI*, 88 (2014) 203.

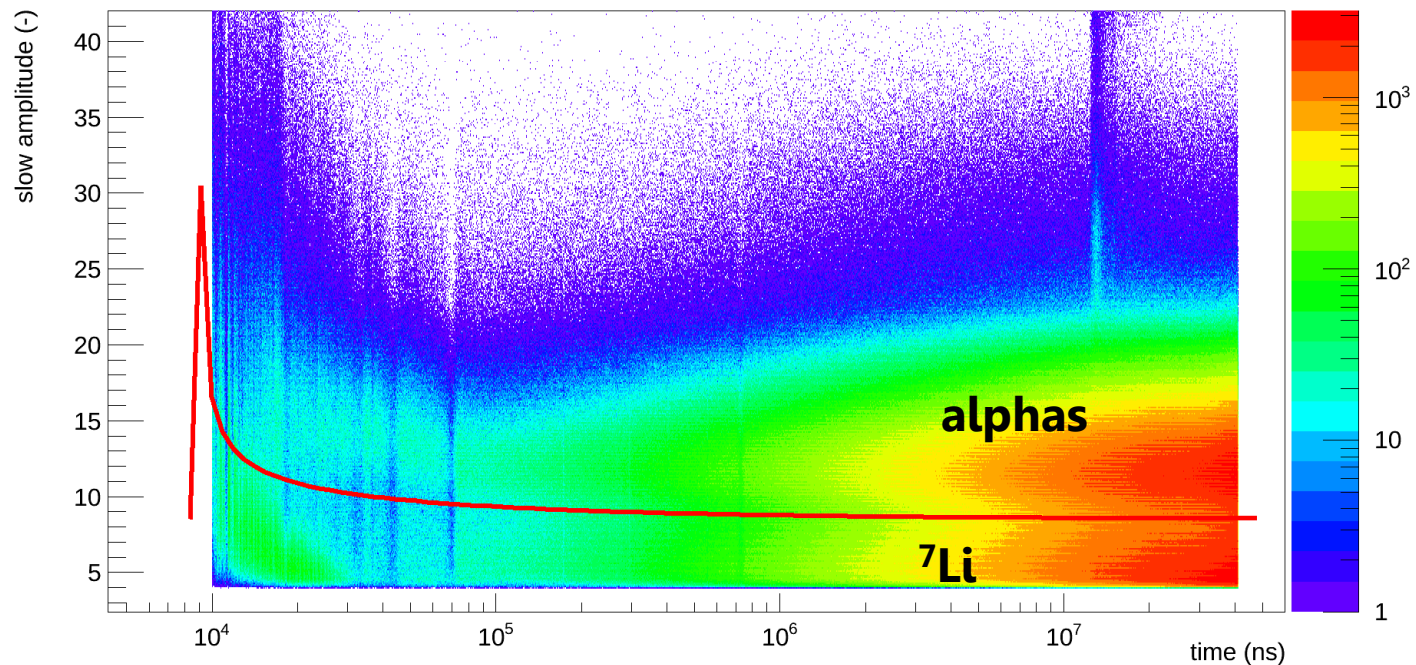
$^{10}\text{B}(n,\alpha)$ used as reference: TOF & Amplitude

Separation between alphas and ^7Li nuclei.

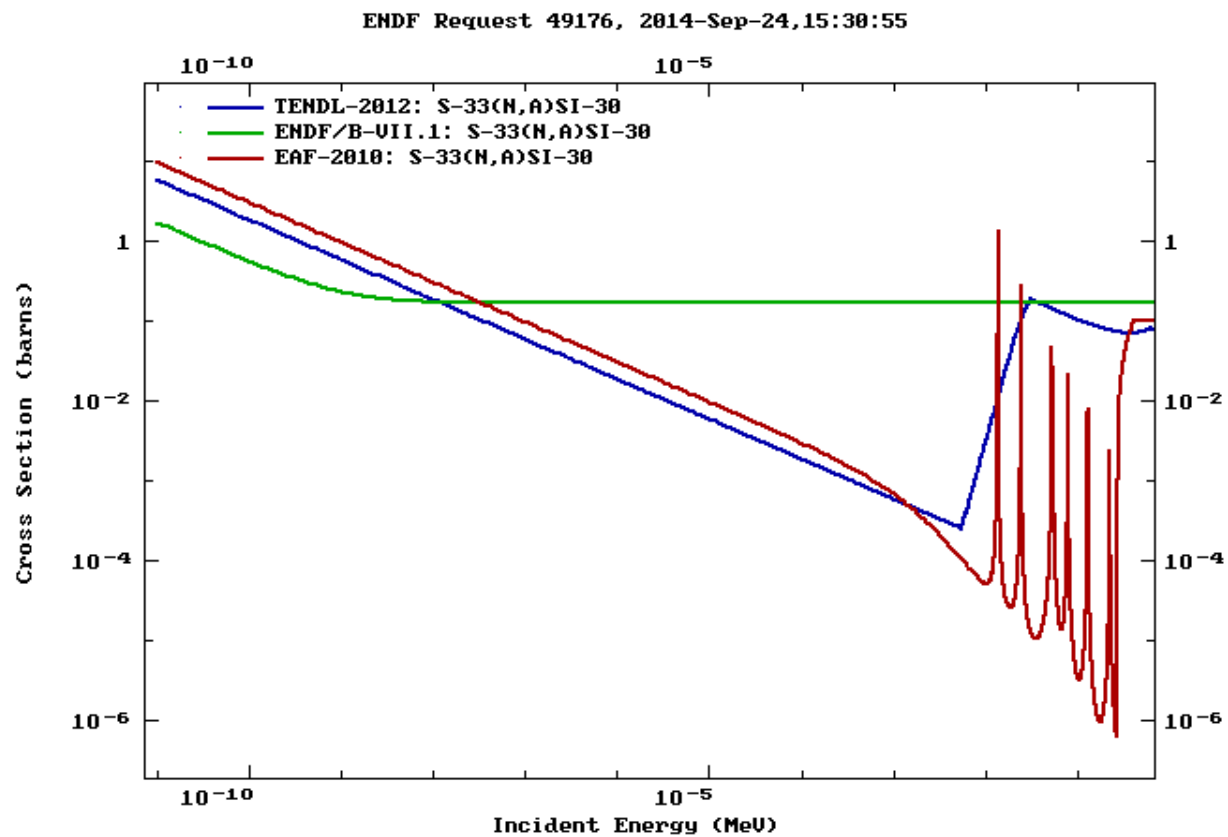
We calculate the alphas lying in the Li peak by means of a Gaussian fit of the amplitude histogram at different energy ranges.

Monte Carlo simulations of the energy deposition.

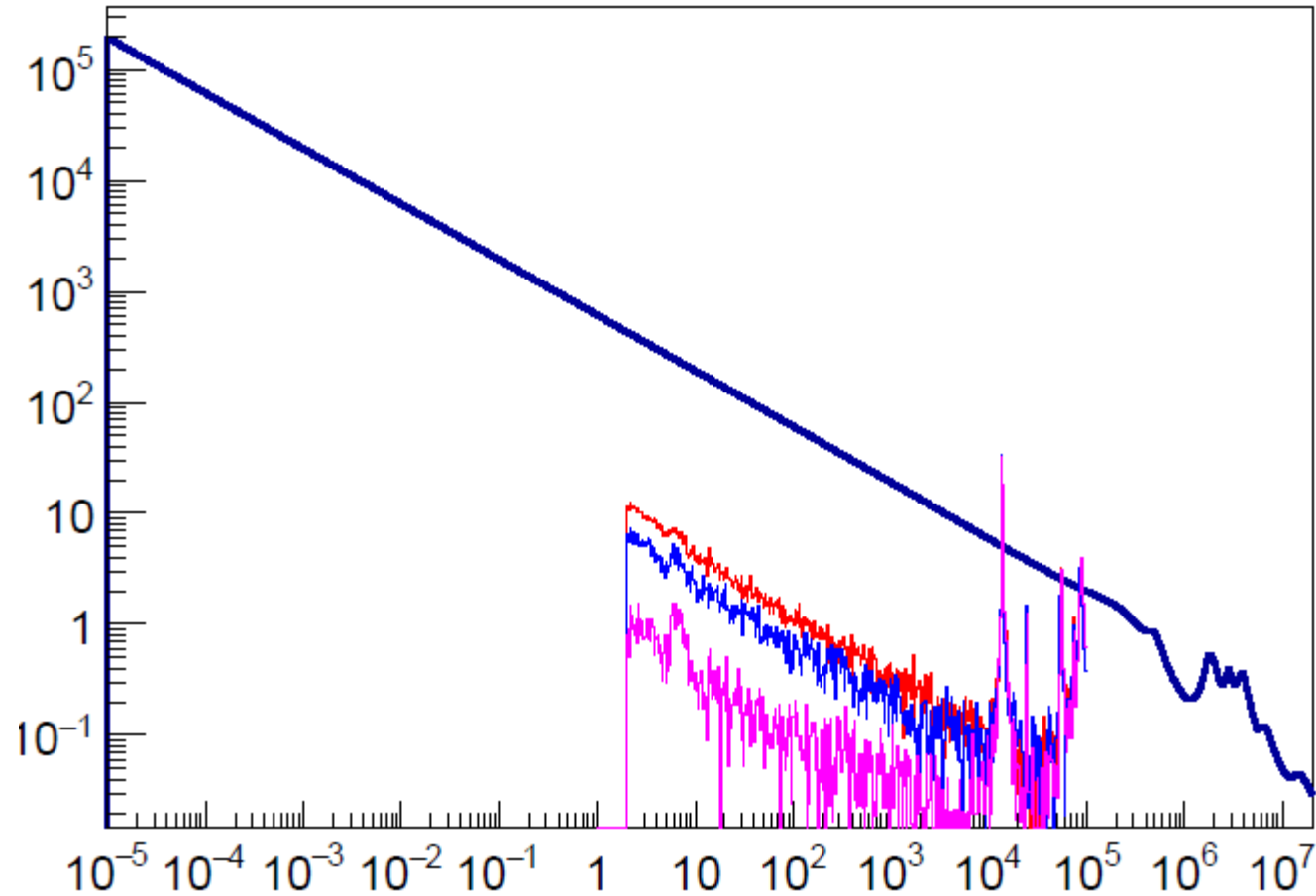
MGAS14_flux__h2_TA_MGAS



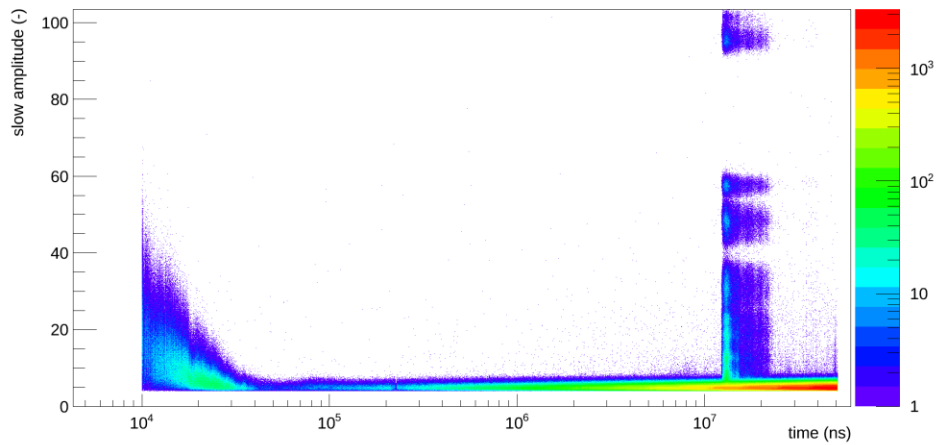
$^{33}\text{S}(n,\alpha)^{30}\text{Si}$ evaluations



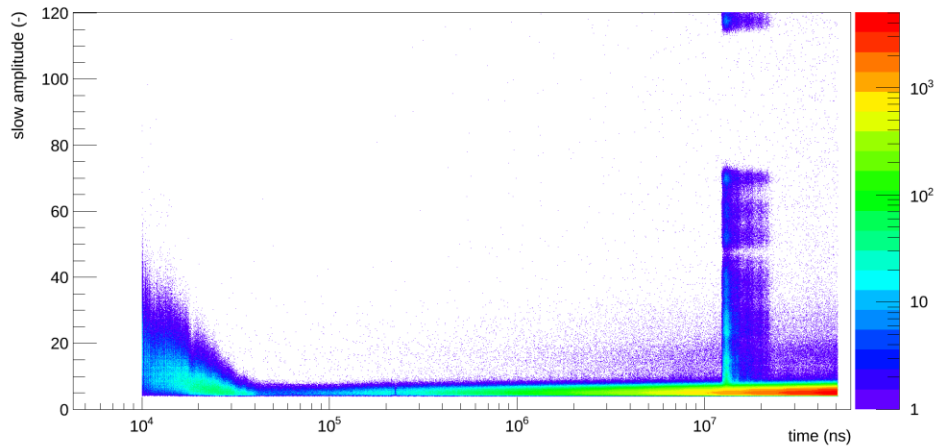
$^{33}\text{S}(n,\alpha)^{30}\text{Si}$ evaluations



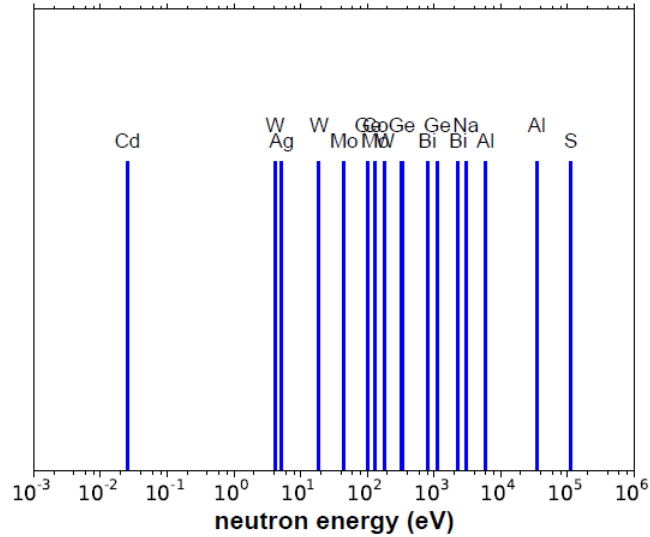
MGAS09_flux_h2_TA_MGAS



MGAS10_flux_h2_TA_MGAS



Positions black resonances



Proposed neutron filters

material	black resonance (eV)	EAR1: thickness (cm)	EAR2: thickness (cm)
C	-	-	-
Cd	thermal cut-off	0.05	0.05
W	4, 19, 184	0.08	>0.8
Ag	5.2	0.05	0.05
Mo	45	0.1	> 1.0
Co	132	0.025	0.025
Bi	800, 2300, γ -flash	> 1.0	> 5.0
Na	3000	-	-
Al	5900, 30000	8.0	> 8.0
S	112000	>8.0	16.0
Pb	γ -flash	1.0 and 2.0	1.0 and 2.0

